NONLINEAR THREE DIMENSIONAL ANALYSIS OF REINFORCED CONCRETE STRUCTURES

Steinar Sandbakk, Dr.Eng.

Multiconsult Narvik A.S.
Division of Concrete Structures.
Norwegian Institute of Technology, Trondheim,
Norway

Keywords: Concrete, Nonlinear Analysis, Tension-stiffening, Aggregate-interlock, Shear, Punching-shear.

ABSTRACT

This investigation deals with nonlinear analyses of reinforced concrete structures. The method of analysis is based on a displacement formulation of the finite element method. A general three-dimensional stress-strain relation is incorporated in the program.

The material model proposed by Niels Saabye Ottosen is employed for the mathematical modelling of the concrete behaviour. The nonlinear behaviour of the reinforcement bar is approximating the usual stress-strain curve of reinforcement steel (see Fig. 5).

Due to the general three-dimensional analysis, the possibility of obtaining three different cracks in the same integration point has been incorporated in the program.

Through the restart technique, variation of the shear transfer across a crack can be accounted for. Tension-stiffening can also be simulated by use of the restart procedure.

Application of the theory is presented for a wide range of numerical examples, namely; 4 different beams with 3 different types of failure, 1 shear panel, 2 slabs exposed to punching shear and 1 shell exposed to punching shear. The numerical results are compared with experimental and analytical results available in the litterature.

1. INTRODUCTION

Great attention has been paid to the development of more accurate methods of analysis for reinforced concrete over the last twenty years. The structural behaviour of reinforced concrete is complex and depends on a number of factors, among which the following will be mentioned:

- the material is made from many constituents; cement paste, sand, larger aggregates and reinforcement bars
- both its strength and stiffness are strongly depending on all stress components, which means that the stress-strain relationship is nonlinear. Deviations from linearity between strains and stresses become more pronounced and even hydrostatic compressive loadings results in non-linear behaviour /1/. In addition, when stresses are compressive, dilatation occurs close to the failure state /2/
- cracking of concrete in tension and crushing in compression
- interaction effects between reinforcement and concrete, such as dowel action in the reinforcement steel, bond slip between concrete and reinforcement steel and aggregate interlocking at cracks.

Great progress has been made over the last ten-fifteen years in developing numerical computational techniques for analysing concrete structures. The finite element method have made it possible to analyse structures of complex geometry and which undergo large nonlinearities.

During 1984-1985 a finite element program has been carried out at the Division of Concrete Structures at NTH /3/. The program works for general three-dimensional stress-states and it pays attention to nonlinearities such as;

- the nonlinear behaviour of concrete in compression, including strain-softening.
- dilatation
- cracks
- nonlinear behaviour of reinforcement.

2. ABSTRACTS FROM CONTINUUM MECHANICS

Considering proportional loading and a given loading rate, a failure criterion for an initially isotropic and homogeneous material in a homogeneous stress state can be expressed in terms of the three stress invariants. Alternatively, the criterion can be given in the form

$$g\ (\sigma_1\ ,\ \sigma_2\ ,\ \sigma_3\ ) = 0 \qquad (1)$$

where σ_1, σ_2, and σ_3 are the principal stresses that occur symmetrically. Tensile stresses are considered to be positive.

It appears to be convenient to use the following three invariants of the stress tensor σ_{ij}:

$$I_1 = \sigma_{ii} = \sigma_1 + \sigma_2 + \sigma_3 \tag{2}$$

$$J_2 = \frac{1}{6}\{(\sigma_1 - \sigma_2)^2 + (\sigma_2 - \sigma_3)^2 + (\sigma_3 - \sigma_1)^2\} \tag{3}$$

$$J = \frac{3\sqrt{3}}{2}\,\frac{J_3}{J_2^{3/2}} \tag{4}$$

$$J_3 = \frac{1}{3}\, S_{ij}\, S_{jk}\, S_{ki}\,, \quad S_{ij} = \sigma_{ij} - \frac{1}{3}\sigma_{kk}\,\delta_{ij} \tag{5),(6}$$

I_1 is the first invariant of the stress tensor, and J_2 and J_3 are the second and the third invariant of the stress deviator tensor, respectively. The often applied octahedral normal stress σ_0 and shear stress τ_0 are related to the preceding invariants by

$$\sigma_0 = I_1/3 \tag{7}$$

$$\tau_0^2 = 2J_2/3 \tag{8}$$

For this purpose, any point, $P(\sigma_1, \sigma_2, \sigma_3)$, in the stress space is described by the coordinates (ξ, ρ, θ), in which ξ is the projection on the unit vector $\mathbf{e} = (1,1,1)/\sqrt{3}$ on the hydrostatic axis, and (ρ, θ) are polar coordinates in the deviatoric plane, which is orthogonal to (1,1,1), see Fig. 1.

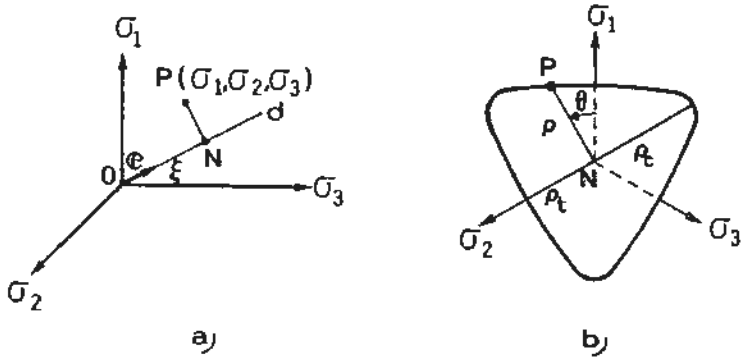

Fig. 1 a) Haigh-Westergaard coordinate system with hydrostatic axis along d
b) Deviatoric plane

The values of the coordinates (ξ , ρ , θ) are given by

$$\xi = I_1 / \sqrt{3} \tag{9}$$

$$\rho = \sqrt{2J_2} \tag{10}$$

$$\theta = \frac{1}{3} \quad \arccos J \tag{11}$$

The failure criterion in Eq. 1 can therefore be expressed more conveniently as

$$f (I_1 , J_2 , \theta) = 0 \tag{12}$$

3. MATERIAL MODEL FOR CONCRETE

Since the program should deal with general three dimensional stress analysis and short time failure the material model proposed by Niels Saabye Ottosen /4,5/ was implemented in the FEM-program. Other reasons for choosing the material model of Ottosen was:

- The model is recommended by CEB./5/
- The model can easily be fitted to different concretes.
- The model is physical complete; i.e.it applies to all stress states including those where tensile stresses are present, and therefore:
- The model is easy to use.

3.1 Failure criterion

The failure criterion proposed by Ottosen /4,6,7,8/ uses explicitly the formulation of Eq. 12 on the form

$$A\frac{J_2}{f_c^2} + \lambda\frac{\sqrt{J_2}}{f_c} + B\frac{I_1}{f_c} - 1 = 0 \tag{13}$$

Where A, B are parameters /3,5/, $\lambda = \lambda(\cos 3\theta)$/3,4/ and $f_c = |f_c|$. Eq. 13 has a simple geometrical interpretation when it is considend as a surface in a cartesian coordinate system with axis σ_1 , σ_2 , σ_3, Fig. 2.

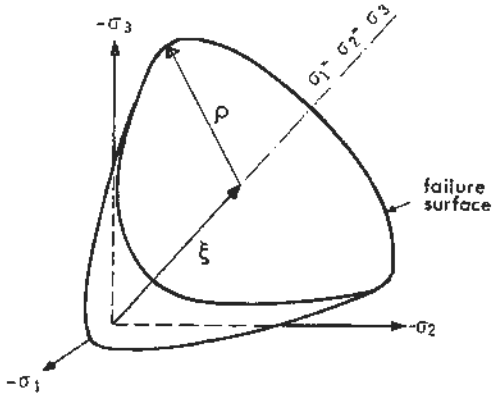

Fig. 2 Schematic representation of the failure surface of concrete in three-dimensional principal stress space.

The characteristics of the failure surface given by Eq. 13 are:

- Only four parameters are used
- The surface is smooth and convex with the exception of the vertex; even when tensile stresses occur.
- The meredians are parabolic and open in the direction of the negative hydrostatic axis.
- The trace in the deviatoric plane changes from nearly triangular to circular shape with increasing hydrostatic pressure.
- It contains earlier proposed criteria as special cases, for instance:
  1) the criterion of Drucker and Prager for A = 0, λ = constant
  2) the von Mises criterion for A = B = 0 and λ = constant.

3.2 Cracking criteria

As the failure criterion proposed by Ottosen applies to all stress states, in term of one equation, it means that another failure criterion must be used to determine the possible existense of tensile cracks. Ottoson's proposal is therefore that cracking occurs, firstly, if the failure criterion is exceeded and secondly, if $\sigma_1 \geq f_t/2$. This is demonstrated in Fig. 3, considering biaxial stress states.

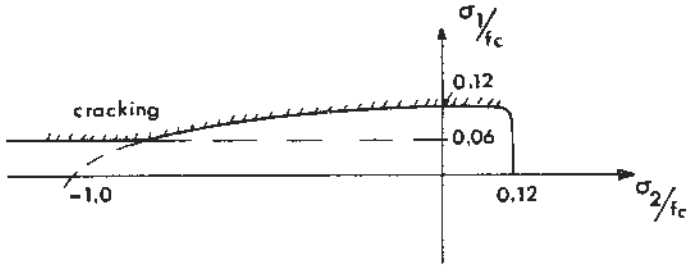

Fig. 3 Cracking criteria

3.3 Stress-strain relations

A convenient measure for the actual load in relation to the failure surface is given by the nonlinearity index β. Having a stress state (σ_1, σ_2, σ_3), the factor β is defined by

$$\beta = \frac{\sigma_3}{\sigma_{3f}} \tag{14}$$

where σ_{3f} is the stress that, along with unchanged σ_1, σ_2 satisfies the failure criterion of Eq. 13.

3.4 Change of the secant value of Young's modulus.

In order to obtain expressions for the secant value of Young's modulus under general triaxial loading, we begin with the case of uniaxial compressive loading. An approximated stress-strain relation is given by /9/

$$-\frac{\sigma}{f_c} = \frac{-A\frac{\varepsilon}{\varepsilon_c} + (D-1)\left(\frac{\varepsilon}{\varepsilon_c}\right)^2}{1 - (A-2)\frac{\varepsilon}{\varepsilon_c} + D\left(\frac{\varepsilon}{\varepsilon_c}\right)^2} \tag{15}$$

ε_c is the strain at max. uniaxial compression strength, i.e. $\varepsilon = -\varepsilon_c$ when $\sigma = f_c$. $A = E_i/E_c$ in which E_i is the initial modulus and E_c is the secant value at max. strength, $E_c = f_c/\varepsilon_c$. D is a parameter which mainly affects the curve in the strain-softening area, see Fig. 4.

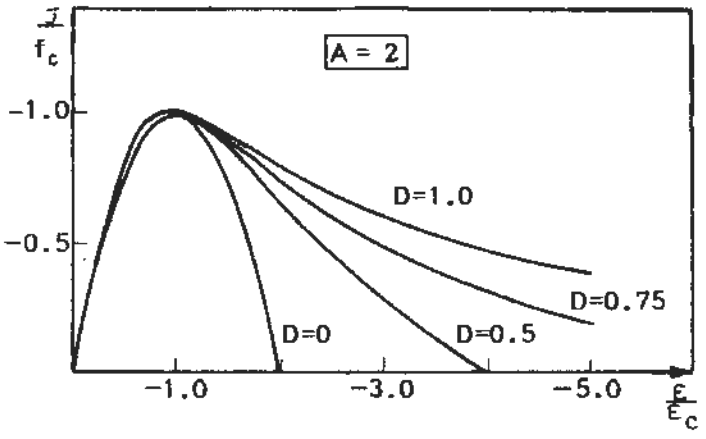

Fig. 4 $\sigma - \varepsilon$ relation for different D-values.

By replacing $-\frac{\sigma}{f_c} = \beta$ and $E_f = E_c$ an expression for the secant E-modulus at the load level β for general triaxial compressive load can be obtained by

$$E_s = \frac{E_i}{2} - \beta\left(\frac{E_i}{2} - E_f\right) \pm \sqrt{\left[\frac{E_i}{2} - \beta\left(\frac{E_i}{2} - E_f\right)\right]^2 + E_f^2\beta[D(1-\beta)-1]} \tag{16}$$

E_c denotes the secant value of Young's modulus at max. uniaxial compression strength and E_f is the secant value at max. triaxial compressive strength.

3.5 Change of the secant value of Poisson's ratio.

As mentioned the program describes the effect of dilatation. Both for uniaxial and triaxial compressive loads the volumetric behaviour is observed as a compaction followed by a dilatation. The expression of υ_s for uniaxial compressive load is therefore generalized to triaxial compressive load by use of the nonlinearity index β

$$\nu_s = \nu_i \quad \text{when } \beta \leq \beta_a \tag{17}$$

$$\nu_s = \nu_f - (\nu_f - \nu_i)\sqrt{1 - \left(\frac{\beta-\beta_a}{1-\beta_a}\right)^2} \text{ when } \beta \geq \beta_a \tag{18}$$

where

ν_i = initial Poisson's ratio

ν_f = the secant value of Poisson's ratio at uniaxial compressive strength.

Only limited knowledge of the increase of υ_s in the strain-softening region exists, but it is an experimental fact that the dilatation continues here. In order to describe this the following procedure is implemented in the program:

For a given change of the secant value E_s, there corresponds a secant value υ_s^* so that the corresponding secant bulk modulus is unchanged. Ottosen decreases the secant value by steps of 5% in the strain-softening region, and to ensure dilatation in this region too, he simply puts $\upsilon_s = 1.005\,\upsilon_s^*$ in each step. In Eqs. 17, 18, a fair approximation is obtained when the following parameter values are applied for all types of concrete

$$\beta_a = 0.8\ , \quad \upsilon_f = 0.36 \tag{19}$$

3.6 Tension cracking.

An important part of the nonlinear behaviour of concrete structures is the development of tensile cracks. A crack is assumed to open at an integration point when a principal stress component exceeds a prescribed tensile limit.

For an uncracked integration point the constitutive relation with respect to principal stresses, can be written as

$$\begin{bmatrix}\sigma_1\\ \sigma_2\\ \sigma_3\\ \tau_{12}\\ \tau_{23}\\ \tau_{31}\end{bmatrix} = \frac{E}{(1+\nu)(1-2\nu)}\left[\begin{array}{ccc|ccc} 1-\nu & \nu & \nu & & & \\ \nu & 1-\nu & \nu & & 0 & \\ \nu & \nu & 1-\nu & & & \\ \hline 0 & 0 & 0 & \frac{1-2\nu}{2} & 0 & 0 \\ 0 & 0 & 0 & 0 & \frac{1-2\nu}{2} & 0 \\ 0 & 0 & 0 & 0 & 0 & \frac{1-2\nu}{2} \end{array}\right]\begin{bmatrix}\varepsilon_1\\ \varepsilon_2\\ \varepsilon_3\\ \gamma_{12}\\ \gamma_{23}\\ \gamma_{31}\end{bmatrix}$$

or

$$\begin{bmatrix}\sigma_1\\ \sigma_2\\ \sigma_3\\ \tau_{12}\\ \tau_{23}\\ \tau_{31}\end{bmatrix} = \begin{bmatrix} D_{11} & D_{12} & D_{13} & 0 & 0 & 0 \\ D_{21} & D_{22} & D_{23} & 0 & 0 & 0 \\ D_{31} & D_{32} & D_{33} & 0 & 0 & 0 \\ 0 & 0 & 0 & D_{44} & 0 & 0 \\ 0 & 0 & 0 & 0 & D_{55} & 0 \\ 0 & 0 & 0 & 0 & 0 & D_{66} \end{bmatrix}\begin{bmatrix}\varepsilon_1\\ \varepsilon_2\\ \varepsilon_3\\ \gamma_{12}\\ \gamma_{23}\\ \gamma_{31}\end{bmatrix} \tag{20}$$

As soon as the cracking criteria are exceeded a crack is formed normal to the σ_1 - direction. Setting $\sigma_1 = 0$ a new stress-strain relation can be expressed by

$$\boldsymbol{\sigma}_L = \mathbf{D}_L \boldsymbol{\varepsilon}_L \tag{21}$$

or

$$\begin{bmatrix}\sigma_1\\ \sigma_2\\ \sigma_3\\ \sigma_{12}\\ \sigma_{23}\\ \sigma_{31}\end{bmatrix} = \begin{bmatrix} \kappa D_{11} & 0 & 0 & 0 & 0 & 0 \\ 0 & (D_{22}-\frac{D_{12}^2}{D_{11}}) & (D_{23}-\frac{D_{21}D_{13}}{D_{11}}) & 0 & 0 & 0 \\ 0 & (D_{32}-\frac{D_{21}D_{13}}{D_{11}}) & (D_{33}-\frac{D_{13}^2}{D_{11}}) & 0 & 0 & 0 \\ 0 & 0 & 0 & \alpha D_{44} & 0 & 0 \\ 0 & 0 & 0 & 0 & D_{55} & 0 \\ 0 & 0 & 0 & 0 & 0 & \alpha D_{66} \end{bmatrix}\begin{bmatrix}\varepsilon_1\\ \varepsilon_2\\ \varepsilon_3\\ \gamma_{12}\\ \gamma_{23}\\ \gamma_{31}\end{bmatrix} \tag{22}$$

This is the stress-strain relation in the local directions. The "κ" - factor is used to prevent an ill-conditioned finite element equation system /4/ and the shear-stiffness parallell to the crack is retained by the shearfactor α ($0 < \alpha < 1$). The material matrix is no longer isotropic and the zeroes in the matrix will not be equal to zero except for the direction of the first crack plane. Therefore the material matrix in an arbitrary direction can be expressed as

$$\mathbf{D}' = \begin{bmatrix} D'_{11} & D'_{12} & D'_{13} & D'_{14} & D'_{15} & D'_{16} \\ D'_{21} & D'_{22} & D'_{23} & D'_{24} & D'_{25} & D'_{26} \\ D'_{31} & D'_{32} & D'_{33} & D'_{34} & D'_{35} & D'_{36} \\ D'_{41} & D'_{42} & D'_{43} & D'_{44} & D'_{45} & D'_{46} \\ D'_{51} & D'_{52} & D'_{53} & D'_{54} & D'_{55} & D'_{56} \\ D'_{61} & D'_{62} & D'_{63} & D'_{64} & D'_{65} & D'_{66} \end{bmatrix} \qquad (23)$$

If the cracking criteria are exceeded once again a second crack will be formed normal to the new σ_1 - direction. By means of $\sigma_1 = 0$ this time too a material matrix corrected for both cracks can be derived,

$$\begin{bmatrix} \sigma_1 \\ \sigma_2 \\ \sigma_3 \\ \tau_{12} \\ \tau_{23} \\ \tau_{31} \end{bmatrix} = \begin{bmatrix} \kappa D'_{11} & 0 & 0 & 0 & 0 & 0 \\ & (D'_{22} - \frac{D'^2_{12}}{D'_{11}}) & (D'_{23} - \frac{D'_{21}D'_{13}}{D'_{11}}) & \alpha(D'_{24} - \frac{D'_{21}D'_{14}}{D'_{11}}) & (D'_{25} - \frac{D'_{21}D'_{15}}{D'_{11}}) & \alpha(D'_{26} - \frac{D'_{21}D'_{16}}{D'_{11}}) \\ & & (D'_{33} - \frac{D'^2_{13}}{D'_{11}}) & \alpha(D'_{34} - \frac{D'_{31}D'_{14}}{D'_{11}}) & (D'_{35} - \frac{D'_{31}D'_{15}}{D'_{11}}) & \alpha(D'_{36} - \frac{D'_{31}D'_{16}}{D'_{11}}) \\ & & & \alpha(D'_{44} - \frac{D'^2_{14}}{D'_{11}}) & \alpha(D'_{45} - \frac{D'_{41}D'_{15}}{D'_{11}}) & \alpha(D'_{46} - \frac{D'_{41}D'_{16}}{D'_{11}}) \\ & \text{sym.} & & & (D'_{55} - \frac{D'^2_{15}}{D'_{11}}) & \alpha(D'_{56} - \frac{D'_{51}D'_{16}}{D'_{11}}) \\ & & & & & \alpha(D'_{66} - \frac{D'^2_{16}}{D'_{11}}) \end{bmatrix} \begin{bmatrix} \varepsilon_1 \\ \varepsilon_2 \\ \varepsilon_3 \\ \gamma_{12} \\ \gamma_{23} \\ \gamma_{31} \end{bmatrix} \qquad (24)$$

If or when cracking takes place in three planes due to redistribution of stresses or further loading, the concrete looses its stiffness. That is, in order to avoid singularity problems as far as stiffness is concerned, the material matrix retains 5 o/oo of its inital value.

3.7 Tension-stiffening.

The tension-stiffening effect is taken care of by varying the non-illconditioning factor, κ , which actually is a measure for the tensile stress transferred across a crack. Use of the restart-technique makes it possible to vary the κ - factor during the load history.

4. STRESS-STRAIN RELATION FOR REINFORCEMENT STEEL

To describe the nonlinear behaviour of the reinforcement steel, a uniaxial relationship between axial stresses and strains in the reinforcement bars is required. For this purpose the stress-strain relation shown in Fig. 5 is used. This idealized model can be adjusted to most of the reinforcement types by varying the five input values shown on the Fig.

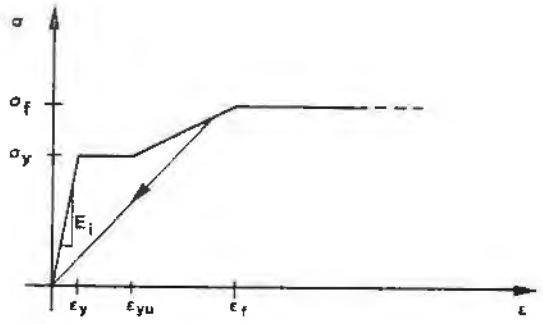

Fig. 5 Stress-strain relation of reinforcement.

5. NUMERICAL STUDIES

In ref. /3/ several numerical analyses are carried out for different concrete structures. The following structures were analysed up until failure and compared to experimental data:

- One beam which failed by yielding of the tensile reinforcement. Two different beams, both failed by diagonal tensile failure or exceeded shear strength. One beam failed by compression failure. Two shear panels. Two concrete slabs exposed to punching shear and one concrete shell exposed to punching shear.

5.1 Beam with failure due to exceeded shear strength.

The simply supported reinforced concrete beam shown in Fig. 6 was tested at Division of Concrete Structures at NTH, during the spring 1984. During the experiment it was observed that the beam failed due to a rapid diagonal crack for a load of 38.6 kN.
The material strengths for concrete and steel was 21.1 MPa and 428 MPa, respectively. Fig. 7 shows the midspan-deflections from both the experiment and the analysis. In the analysis the shear factor was varied as shown on the Fig. This gave a failure load of P = 40 kN while the failure load for α (= SRF) = constant was 46.5 kN.
The same failure-load-reducing-effect is referred by Arnesen et.al. /10/ in 1980, and it is caused by the almost complete loss of stiffness in the integration points where two cracks are formed. The calculated crack pattern is shown in Fig. 8 and the double cracked integration points indicate the complicated stress distribution that is present when shear load is

considered. At the last converged load level P = 40 kN, compression failure was obtained in the top of the beam near the load, see *). This underlines the importance of a realistic constitutive modelling in the strain-softening region.

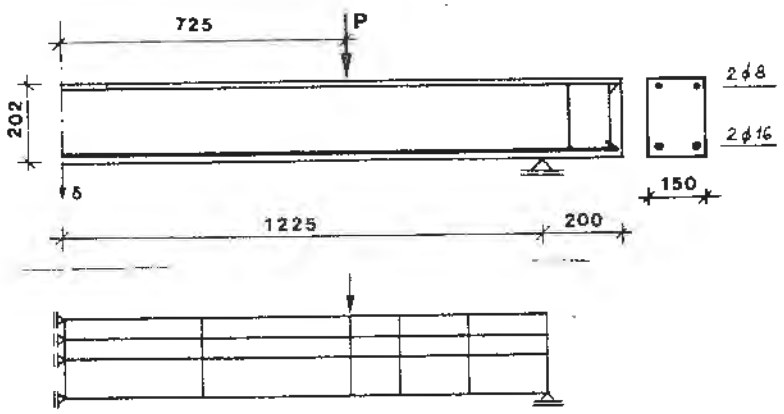

Fig. 6 Laboratory beam and element model.

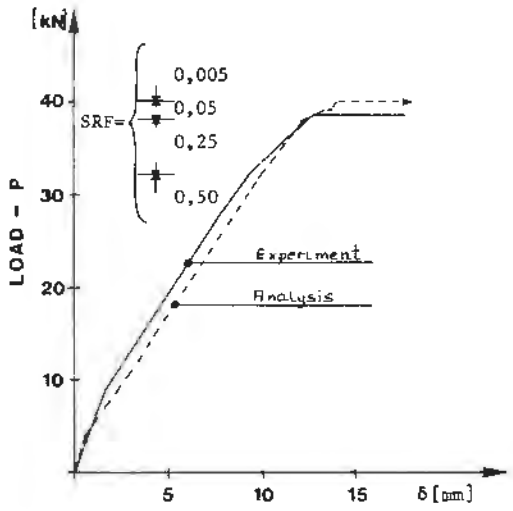

Fig. 7 Load-deflection due to varying SRF-factor

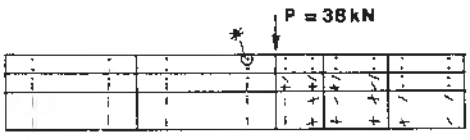

Fig. 8 Calculated crack pattern.

5.2 Monotonically loaded reinforced shear panels.

Fig. 9 shows one of the shear panels tested by Cervenka /11/ and the corresponding element model used in the present analyses. The smeared reinforcement used in the test specimen is in the analyses replaced by three reinforcement bars in each concrete element.

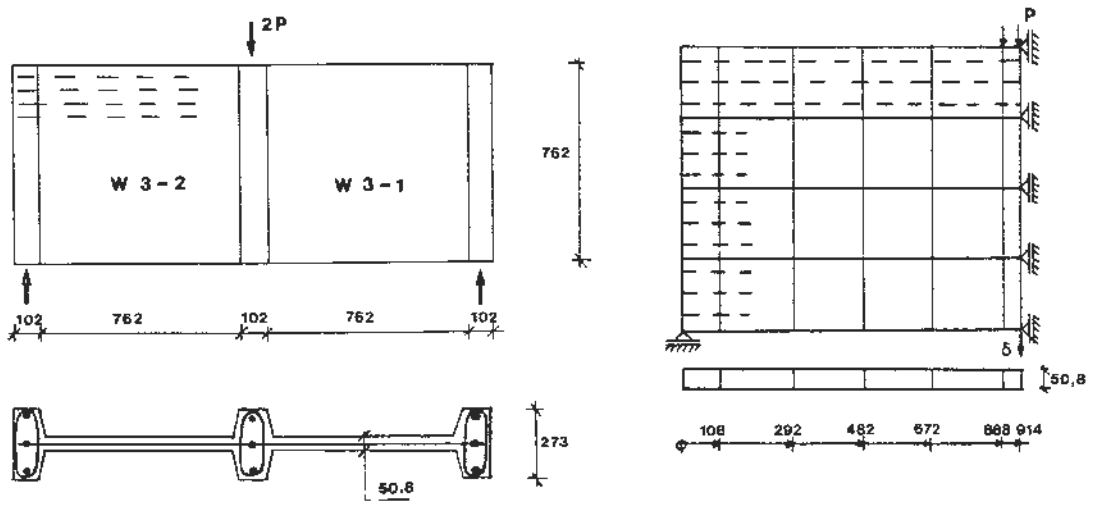

Fig. 9 Test specimen and element model.

The load-deflection curve from the experiment is shown as the solid line in Fig. 10a-c. The almost horizontal level just before failure indicates a plastic behaviour in either the concrete or the reinforcement. Both Sørensen's results /12/ and the present study gave tensile yielding in the reinforcement which, along with the experimental tests, indicate that the shear and the bending capacity of the panel are very close to each other.

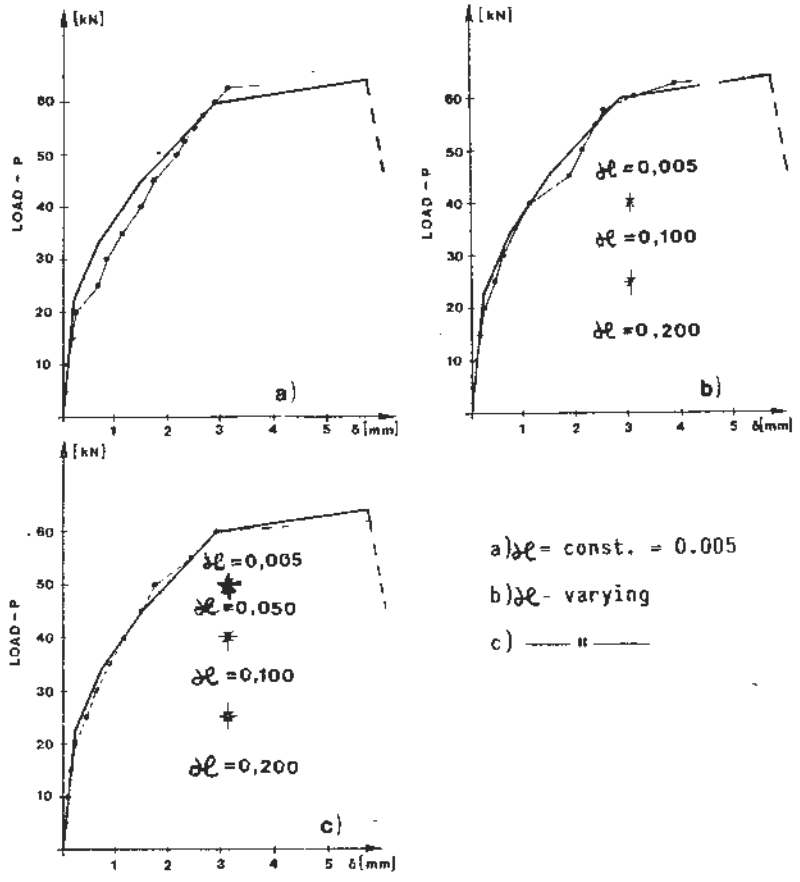

Fig. 10 Three different analyses compared to the experiment.

Three program runs were done in order to examine the material model's ability of describing the behaviour of the panel during proportional loading, and the load-deflection curves at the midspan are shown in Fig. 10.

Two of the three runs make use of an "artificial" way of taking tension-stiffing effects into account, see Ch. 3.6. Because of the possibility of load incrementation the factor κ can be varied through the load history. All three runs gave good agreement between the theoretical approach and the real behaviour of the panel. As expected, a stiffer behaviour was obtained for levels around service loads when tension-stiffening was taken into account. In fig. 10c a minor reduction of the failure load can be observed. This effect is also pointed out by Leibengood et.al. /13/, considering tension-stiffening. Fig. 11 shows the calculated and the experimental crack pattern and a concentration of double-cracked intergration points can be observed along the compression diagonal. This indicates a failure crack similar to the experimental failure crack.

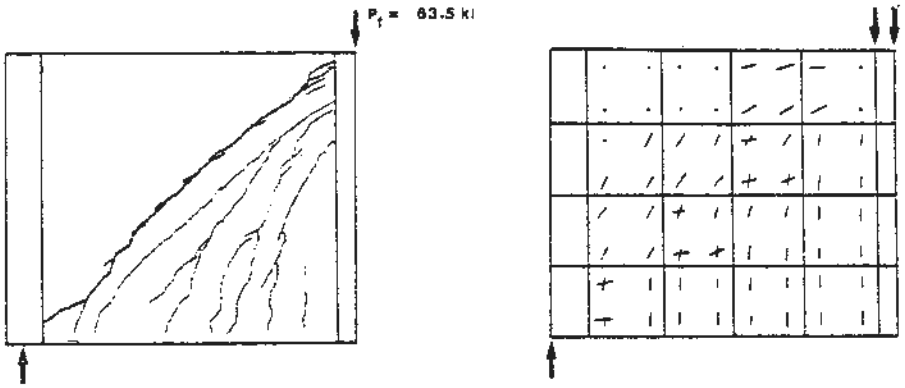

Fig. 11 Experimental and calculated crack pattern.

5.3 Reinforced concrete slabs exposed to punching shear.

Fig. 12 shows a test specimen testet in the laboratory at the Division of Concrete Structures at NTH /14/. Two different support conditions were used in the laboratory, one fixed against horizontal displacements and one free, see Fig. 13. Only a quarter of the slab was modelled and the element model used in the analyses is shown in Fig.14.
Three different program runs were carried out in order to examine the analytical behaviour of the simply supported slab, and the result is shown in Fig. 15 as the load-deflection curve of the centre of the slab. Compared to the experiment curve a) shows a very ductile behaviour of the slab after two cracks had occured in the same integration point. A double crack will seldomly exist in a test specimen, which means that the stiffness is maintained in two of the three directions. To avoid this damaging loss of stiffness, the κ factor was increased.
A low value of $\kappa = 0.05$ gave considerable better results what stiffness and failure load concern, see curve b) in Fig. 15.
In order to examine the influence of the support conditions on the stiffness, two analyses were carried out. In the first run the supports were fixed against horizontal displacements.

This gave a too stiff behaviour at higher load levels, while the initial stiffness was very close to the stiffness of the experiment, see curve b) in Fig. 16. In an experimental test a certain displacement is required in order to establish the fixed support conditions. Therefore it is obvious that the fixed support at the bottom of this slab gives a to stiff behaviour in the analyses. Due to this the middle plane of the slab was fixed against horizontal displacements in the second run, which is shown in Fig. 16, curve c.

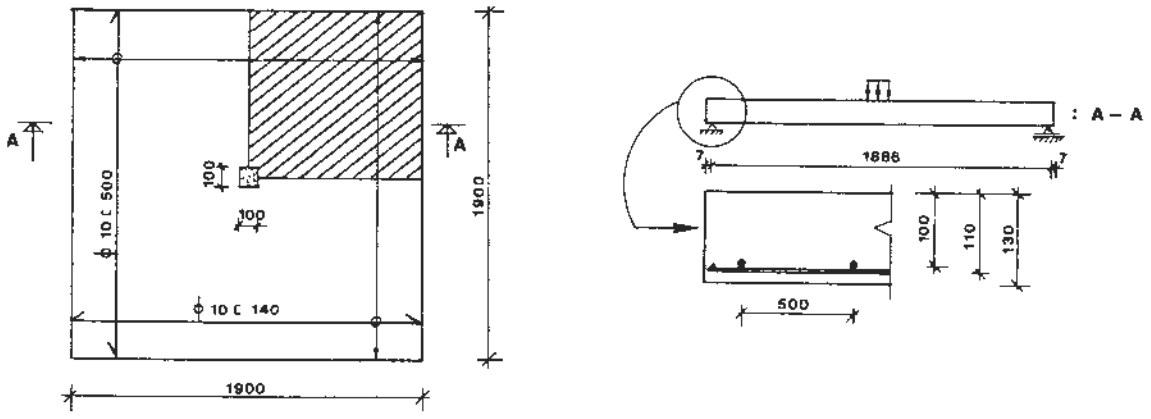

Fig. 12 Geometry of the laboratory slab.

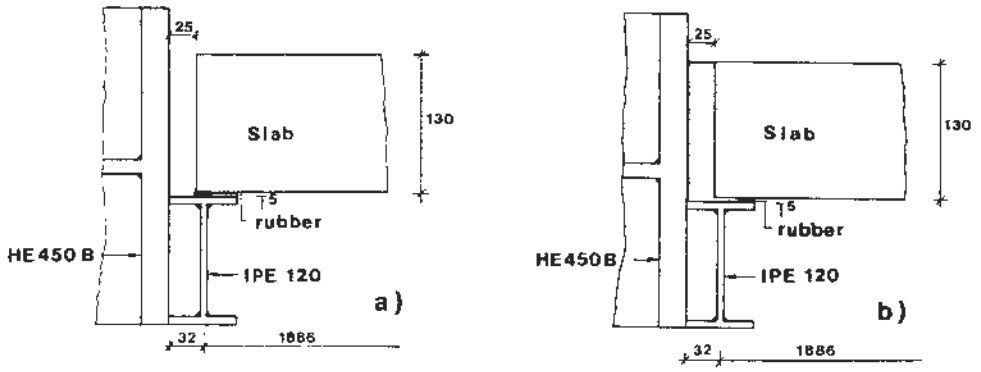

Fig. 13 Support conditions a) Simply supported
b) "Fixed"

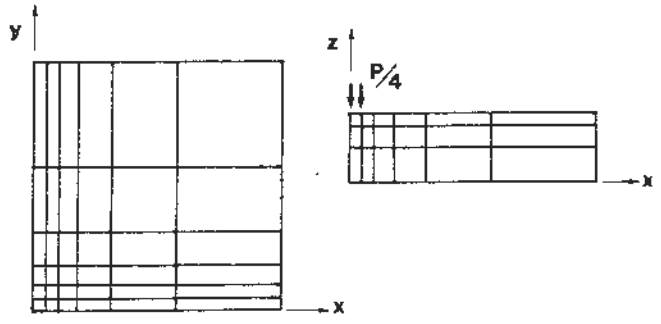

Fig. 14 Finite element model

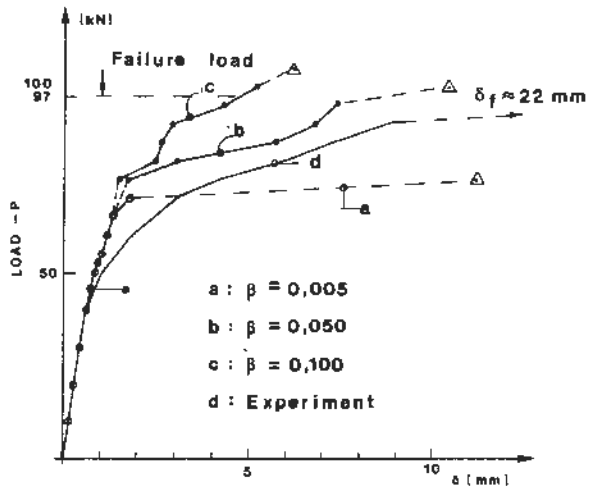

Fig. 15 Load-deflection curve simply supported slab compared to three program runs.

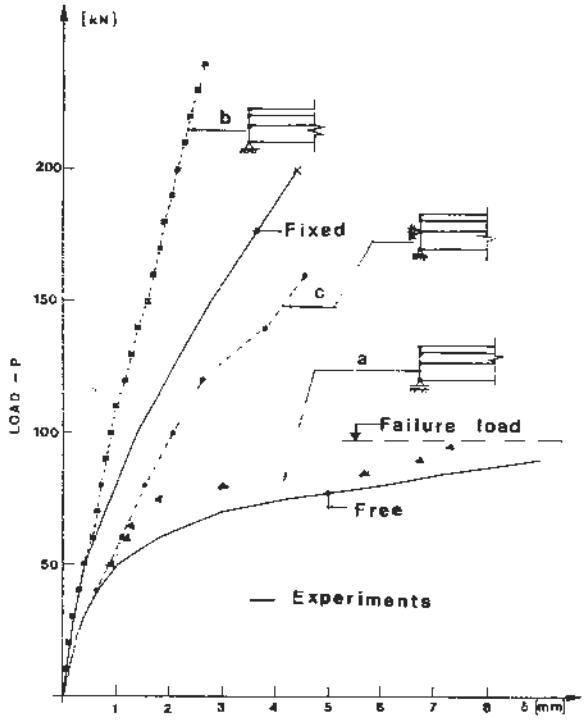

Fig. 16 Present analysis compared to the load-deflection curves of the experiments.

Based on these results it is reason to believe that the real support conditions are somewhere beetween the two examples. This indication is also supported by the fact that a small rotation of the flange of the supporting steel beam was observed during the experiment.

6. CONCLUSIONS

Not much experience have previously been gained with general nonlinear three-dimensional analyses and the finite element approach. However, the present study shows that these kind of analyses are well suited for numerical implementation in the finite element method.

The experience of the present work gives full support to the previous recommendation /5/ of the material model proposed by Ottosen, when nonlinear behaviour of concrete structures is considered.

Structures as shells, arches and continous slabs that carry much of the loads via compression arches, needs more reflection when considering and making the supports, than beams. The present study underlines also the importance of choosing the right support conditions when analysing punching shear. It also confirms the known effect of strongly increased punching shear strength when the support conditions are getting more and more fixed.

The technique with reduced shear factor gives good results when analysing shear problems in beams without stirrups. In elements without reinforcement α has a greater influence of the stiffness.

Tension-stiffening through the factor κ has a positive influence of the stiffness at the level of service load. When analysing two-dimensional problem however, it may reduce the failure load in some examples. It has also a positive effect when analysing three-dimensional problems, as correction for the total loss of stiffness when two cracks occur in the same integration point.

REFERENCES

1. Green, S.J. and Swanson, S.R. (1973): " *Static Constitutive Relations for Concrete*". Air Force Weapons Laboratory, New Mexico. Techn. Report no. AFWL-TR-72-244 (AD 761820).

2. Brantzæg, A.: *"Failure of a Material Composed of Nonisotropic Elements"*. Det Kongelige Norske Videnskabers Selskabs Skrifter 1927 nr. 2.

3. Sandbakk, S.: *"Nonlinear Three Dimensional Analysis of Reinforced Concrete Structures"*. Doctoral dissertation. Division of Concrete Structures. The Norwegian Institute of Technology, Trondheim 1985.

4. Ottosen, N.S.: *"Nonlinear Finite Element Analysis of Concrete Structures"*. Risø National Laboratory, Denmark. Risø-R-411. 186 p. May 1980.

5. Eibl, J. et al.: *"Concrete under Multiaxial States of Stress. Constitutive Equations for Practical Design"*. CEB-Bulleting No.156, Juni 1983.

6. Ottosen N.S.: *"Failure and Elasticity of Concrete"*. Risø National Laboratory, Denmark. Risø-M-1801. 67 p,1975.

7. Ottosen, N.S.: *"A Failure Criterion for Concrete"*. Journal Eng. Mech.Div. 1977, ASCE 103, pp. 527-535

8. Ottosen, N.S.: *"Constitutive Model for Short-Time Loading of Concrete"*. Journal Eng. Mech.Div. 1979, ASCE 105, pp. 127-141.

9. Sargin, M.: *"Stress-Strain Relationship for Concrete and the Analysis of Structural Concrete Sections"*. University of Waterloo, Canada. Solid Mechanics Division SM Study No. 4 pp. 23-26.

10. Arnesen, A., Sørensen, S.I. and Bergan, P.: *"Nonlinear Analysis of Reinforced Concrete"*. Computers and Structures, Vol. 12 pp. 571-579, 1980.

11. Cervenka, V.: *"Inelastic Finite Element Analysis of Reinforced Concrete Panels"*. Ph. D. Dissertation, Dept. of Civil Enginnering, Univ. of Colorado, Boulder 1970.

12. Sørensen, S.I.: *"Nonlinear Finite Element Analysis of Plane Stress Problems in Reinforced Concrete"*. Div. of Concrete Structures, Norwegian Institute of Technology, Trondheim, Norway,May 1981.

13. Leibengood, L., Darwin, D. and Dodds, R.H.: *"Tension Stiffening and Compression Softening in Concrete"*. Recent Advanses in Engineering Mechanics and Their Impact on Civil Engineering Practice, Vol. 2 1983 pp. 1046.

14. Bjerkeli, L.M., Ekeberg, P.K. and Meaas, K.: *"Gjennomlokking av plater"*. Dinploma Work 1980 at Division of Concrete Structures, NTH, Norway.